# Electrical Design of Composite Bus Post Insulator up to 400kv

**P Sreeram Sunil varma**
M.Tech Student
Department of EEE
UCEK (A), JNTUK, Kakinada
Email:sriramsunilvarma@gmail.com

**K Sri Kumar**
Assistant Professor
Department of EEE
UCEK (A), JNTUK, Kakinada
Email: kotni.77@gmail.com

**B Gunasekaran**
Technical Head
Deccan Enterprises Ltd
Hyderabad
Email: bgunasekaran@deccan.in

***Abstract*— Insulators are key components in power system and play an important role in reliable transmission of electric power. Composite insulators are extensively used in the transmission network, due to their improved pollution performance. For satisfactory long term performance, the electric stress on the insulator needs to be below an acceptable level. In this paper, the electric field distribution along the composite post insulators of voltage ratings 11kV - 400kV are studied using a Commercially available Three - Dimensional software based on the Boundary Element method (BEM). The effect of various design parameters and the dimensions of the grading ring, on the distribution of electric field are reported.**

## I. INTRODUCTION

The use of polymeric insulators has increased recently due to their advantages over the conventional porcelain and glass insulators. Excellent contamination and wetting performance, high ratios of strength to weight, vandalism resistance, easy transport and installation over conventional ceramic insulators, especially in Extra High Voltage (EHV) and Ultra HV lines made the utilities opt for composite insulators. [1]. However, as observed in every product, they suffer from certain drawbacks which can be eliminated with careful design. The composite insulators need to pass stringent tests before installed into service, to guarantee the in - service performance of the insulators.In addition, the electric stress on all parts of the insulator has to be kept low, to maintain the excellent hydrophobic properties of the housing.

In long rod insulator or insulator strings, the position of highest E-field occurs adjacent to the energized end fitting. When a grading ring is employed on the energized end, the position of highest electric field gets shifted and the field is reduced. Electric Power Research Institute (EPRI) suggests the critical values for the following critical regions [2].

- Internal to the fiberglass rod and rubber weathershed material: 3 kV/mm.
- Surface E-field magnitudes on weathershed material: 0.45 kV/mm (rms) measured 0.5 mm above the surface of the sheath.
- Surface E-field magnitudes on the metallic end-fittings and corona rings: These should be controlled such that the unit passes the corona / radio interference test. A surface gradient of 2.1 kV/mm is taken as acceptable limit.

It is important to reduce the high value of electric field near the energized end region so as to prevent corona discharges, internal discharges in fiber glass rod, dry band arcing which leads to tracking on the weathershed material which can impact the service life and performance of the composite insulators.

Although electric field can be measured using live line testers [3] and optical electric field sensors [4] these need to be calibrated regularly as per the IEEE 644 [5]. Also a prototype model needs to be built for the study, which would be costly and impractical during the design phase of the insulator. With the advent of modern computing, various software are available [6] for efficient calculation of the electric field and voltage distribution along the insulators.

This paper presents the work done on the composite post insulators of voltage ratings namely 11kV, 33kV, 66kV, 132kV, 220kV & 400kV. Boundary element method (BEM) was chosen for the work due to its advantages for this particular application when compared to other methods [7]. A Commercially available three - dimensional software based on BEM [8] was used for this study.

## II. INSULATORS MODELED

The composite insulators modeled and the dimensions of the insulators are shown in table 1.

The following considerations were taken as suggested by T.Zhao et al. [9]:

- The Weather sheds of complete insulator were omitted except for the two pitches at the live end and ground end.
- The bus bar was simulated by a cylindrical rod of length 1.6 times the total length of the insulator. The diameter of the bus bar taken was 50 mm for 11kV & 33kV and 100 mm for the remaining insulators.
- The complete (360º) insulator in 3-D was modeled.

The voltages applied were the r.m.s values of the highest Phase to ground system voltages i.e.7kV; 21kV; 42kV; 84kV; 141kV; 242kV for the respective voltage ratings from 11kV - 400kV.

The relative permittivity of the material considered were Fiber glass reinforced plastic (FRP) - 4.0; Silicone Rubber (SiR) - 3.45; and EN8 Steel - 1. The relative permittivity values were taken from respective material manufacturers catalogs.

Table 1: The dimensions of the insulators solved

| Dimensions of the models solved | | | | |
|---|---|---|---|---|
| kV Rating | Creepage Distance (mm) | Total Insulator height (mm) | Flange Diameter (mm) | |
| | | | Top | Bottom |
| 11kV | 464 | 264 | 86 | 86 |
| 33kV | 1024 | 500 | 105 | 105 |
| 66kV | 2421 | 770 | 164 | 164 |
| 132kV | 4606 | 1500 | 164 | 224 |
| 220kV | 7829 | 2300 | 164 | 294 |
| 400kV | 13020 | 3650 | 164 | 294 |
| | | | 294 | 340 |

## III. ELECTRIC FIELD STUDY

The maximum values from the graph plots were taken which are then compared to the critical field values as specified by the EPRI.

In all the insulators the electric field between the triple - point and the bottom of the first shed was maximum. These insulators were simulated with mould over end fitting design in which the Silicone rubber partially covers the end flange. Only the 11kV insulator had Room Temperature Vulcanizing (RTV) sealant applied between End flange and silicone rubber.

In the case of 132kV insulator the critical field values exceeded at the region near the first shed. Different models were simulated by changing the end fitting design and the shape of the Sheath to reduce the field values to be within the maximum permissible limits. In the case of 220kV insulator, two types of grading rings were simulated, to study their effect on the electric field. The 400kV insulators were simulated with different grading rings and with different dimensions.

## IV. RESULTS

The results obtained for the different Post insulator ratings for the critical regions considered in table 2 are shown in the following figures 1 through figure 5. The maximum electric field values obtained in each location is plotted in the bar charts with the maximum permissible value marked for indication.

| Location | | |
|---|---|---|
| 1 | Triple Junction HV side | (a) On Point |
| | | (b) 0.5mm Away towards Air |
| 2 | Weather shed Material | (a) 0.5mm away from housing-Triple point to bottom of 1st Shed |
| | | (b) On Line 0.5mm Above the Sheath HV to GND |
| | | (c) 0.5mm away from housing – Along total Creepage Simulated |
| 3 | Internal to FRP Rod | (a) Along Length from HV to GND at Mid Point of FRP Rod |
| | | (b) Along FRP Rod on Diameter interfacing SiR HV to GND |
| 4 | Internal to Weather Shed Material | Along Length from HV to GND at Mid Point of Sheath |
| 5 | Surface of Metal End Fittings & Grading Ring | (a) On the Surface of the End Flange HV Side |
| | | (b) On the Surface of the End Flange GND Side |
| | | (c) On the Surface of the Grading ring |
| 6 | Tip of Sheds | Along Line joining the Tip of Each shed type (HV to GND) |

2: The Critical regions considered for Electric Field calculations

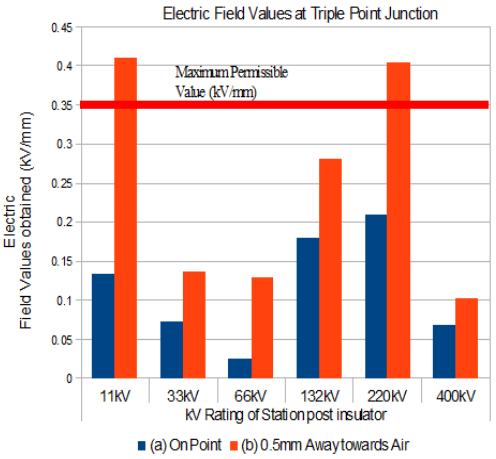


Figure 1: The results and the maximum permissible values for the location 2

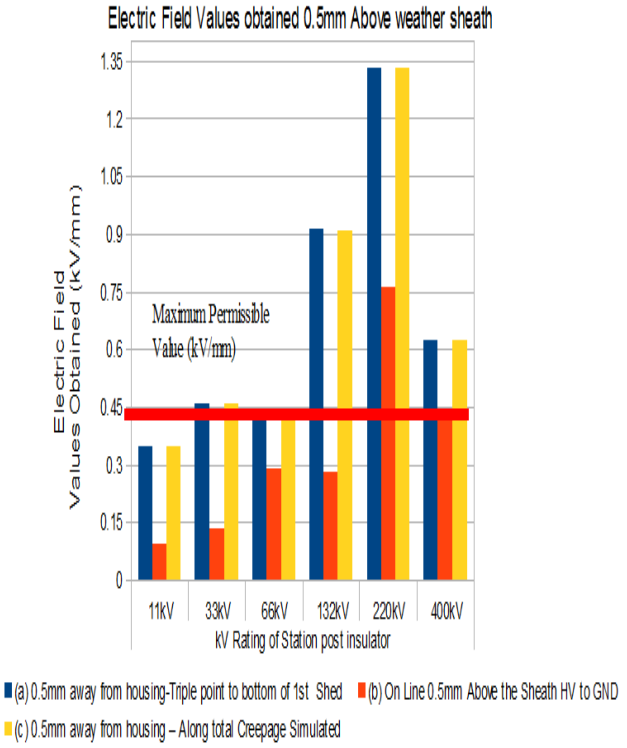


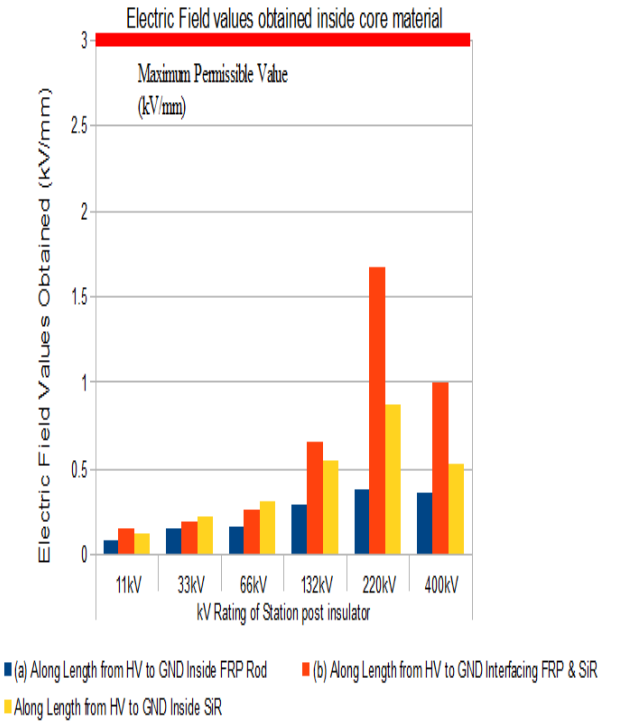


Figure 2: The results and the maximum permissible values for the location

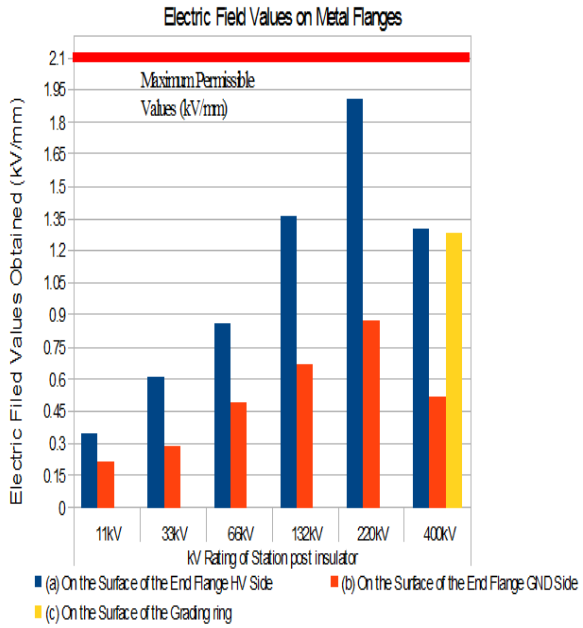


Figure 3: The results and the maximum permissible values for the location 5

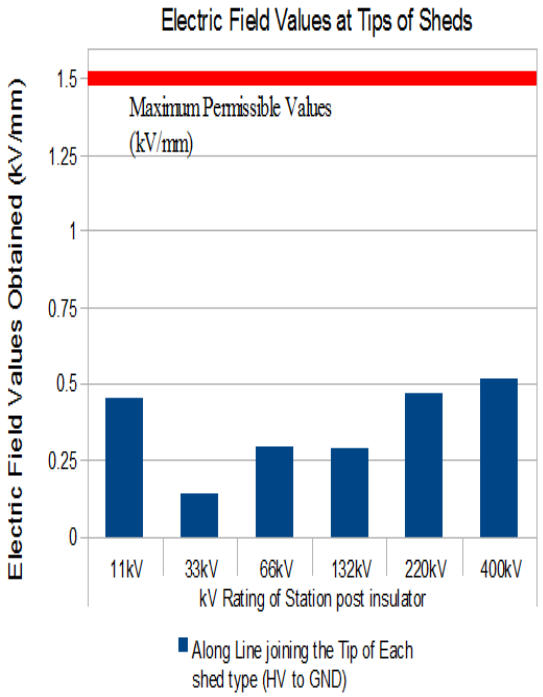


Figure 4: The results and the maximum permissible values for the location 6

The highest electric field generated was around the region between the triple - junction and first shed. In order to better visualize the high values of electric fields, an arrow plot is used as shown in figure 6. The arrow plot is modified to show only the values between 0.35kV/mm to 0.91kV/mm which was the highest value obtained in case

of the 132kV insulator.

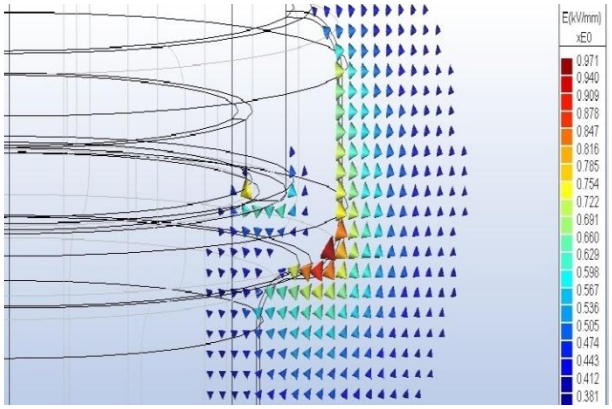


Figure 5: The Arrow plot depicting the highest electric field regions

In order to reduce the electric fields in the region, modifications to the end flange and the SiR sheath were done, 14 Prototypes were simulated with changes in both end flange and the SiR Sheath. The initial design and the final design are presented for reference in figure 7.

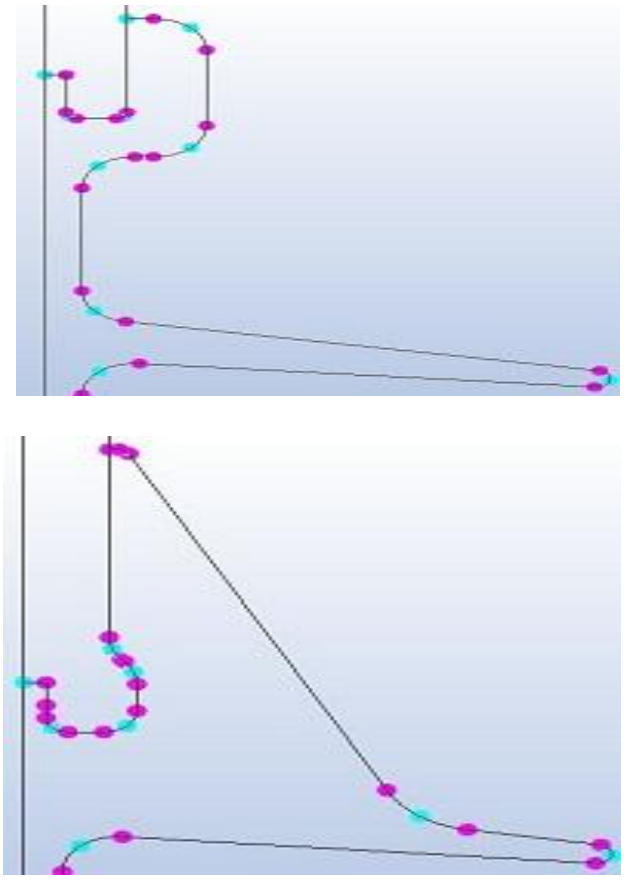

Figure 6: The intial design and final design for 132kV insulator.

In case of the different prototypes simulated for 132kV all the other values are within limits except the region between the End flange and the first shed, the region 2(a) in table1. The variation of the values at the region 2(a) in table 2 for 14 different prototypes simulated are shown in figure 8.

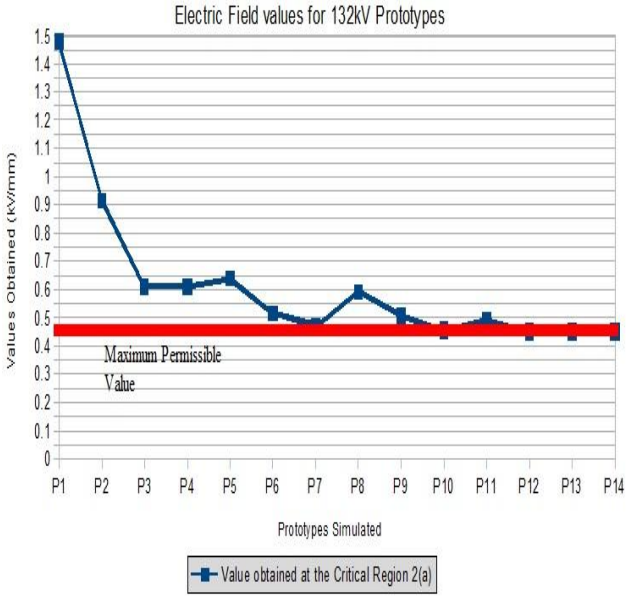


Figure 7: The different field values obtained for 132kV prototypes in the location 2(a)

The electric Field values obtained for the initial and final designs of 132kV insulator are

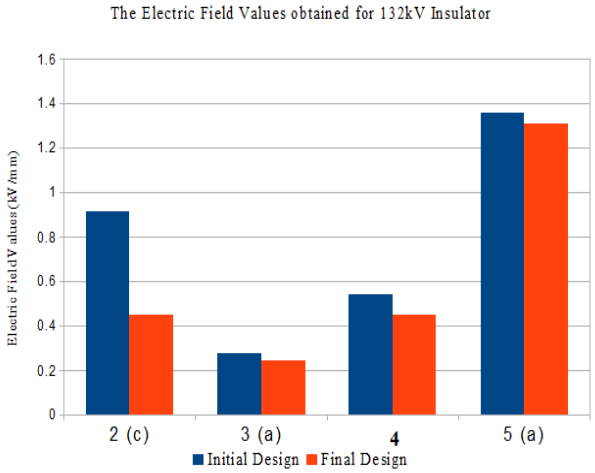


Figure 8: The Electric Field Values for initial and final designs of 132kV insulator

In case of the 220kV insulator, to control the electric field, grading rings were used and two types of grading rings were simulated shown in figure 10.

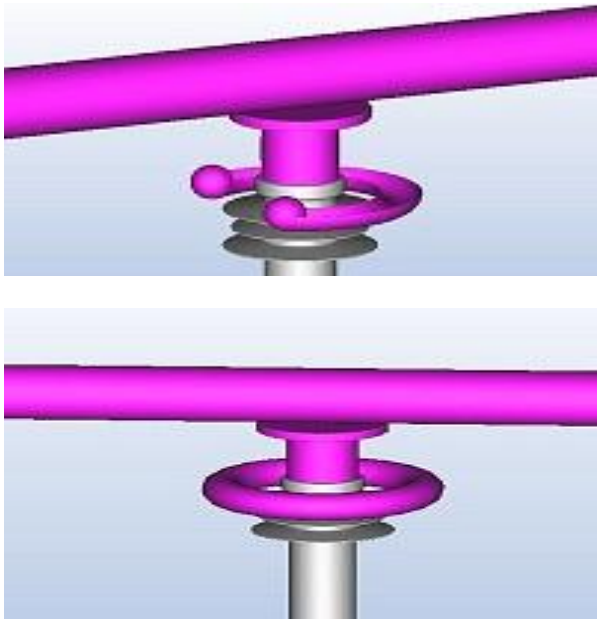

Figure 9: The two types of grading rings used for 220kV insulator.

The Electric field values in critical regions were controlled below the maximum permissible limits with the inclusion of grading rings. The electric filed values for the initial and final prototypes calculated are shown in figure 11. The prototype with closed grading ring showed better results when compared to the open grading ring. The curved outer surface of the grading ring was in line with the first shed as suggested in [10]. A total of 5 different prototypes were simulated for 220kV insulator.

Figure 11 shows the electric field values obtained for initial and final prototypes of 220kV

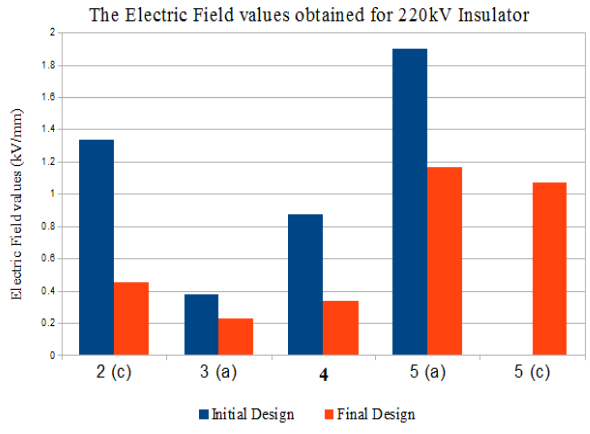


Figure 10: The results for 220kV Prototypes

In case of the 400kV insulator, the grading rings were modified with different dimensions of outer radius and the radius of the tube. The diameters were increased and the model simulated to check for the electric field values. All the grading rings used were closed tubes (toroids) and they were placed in such a way that the curved outer surface was in line with the first shed. A total of 4 different prototypes were simulated for 400kV insulator insulator at various locations mentioned in table 2.

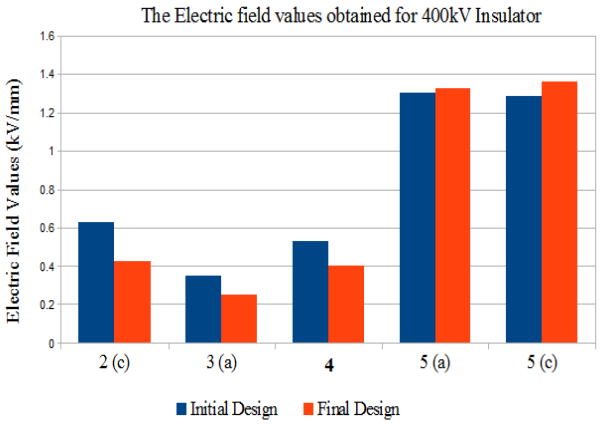


Figure 11: The results for the 400kV Prototypes

## V. CONCLUSIONS

This paper presents the electric field values obtained for the post insulators from 11kV upto 400kV. Also modification to design were done so that the field values in the critical regions are brought down to the permissible limits.

In case of the 132kV insulator, the modification of the design by making the end flange more rounded and also redesigning the SiR sheath over the end flange resulted in controlling the electric fields in critical regions.

Two types of grading rings were simulated for the 220kV insulator and the better one was determined based on the electric field distribution values.

Different grading rings were used with 400kV insulator to get the field below the maximum permissible limits. It can be observed that as the diameter of the grading ring increases the grading of the electric field also becomes better.

## ACKNOWLEGMENT

The Authors wish to thank the management of Deccan Enterprises Limited for using the three dimensional software and permitting to publish this paper.

## VI. APPENDIX

Boundary Element method:

For electrostatic field problems, the governing Poisson equation is to be solved,

$$\delta\phi^2 = -(\rho/\epsilon) \quad \text{eq (1)}$$

Where ϕ is the scalar potential; ρ is the charge density; ε is the permittivity of the medium. The electric field strength E is determined by the gradient of φ ,

$$E = -\Delta\phi \quad \text{eq (2)}$$

For a point source in space, the electric field strength of an observation point has a component in the direction connecting the source point and the observation point. If the potential of an arbitrary reference is set to zero at infinity, the medium in the problem domain is linear and isotropic, and there are more than one source points in the domain, the potential of the observation point can be determined by eq:3,

$$\phi_p = \sum_{k=1}^{n} \frac{q_k}{4\pi\varepsilon}\left(\frac{1}{r_k}\right) \quad \text{eq (3)}$$

where $\phi_k$ is the potential of the observation point; n is the number of the source points; $r_k$ is the radial distance from the source point k to the observation point; $q_k$ is the impressed charge of source k .

Similarly, for a continuous distributed surface or volume source, the potential can be determined by eq:4 or eq:5,

$$\phi_s = \int_s \frac{\sigma_s + \sigma_{es}}{4\pi\varepsilon}\left(\frac{1}{r_s}\right) ds \quad \text{eq (4)}$$

$$\phi_v = \int_v \frac{\sigma_v}{4\pi\varepsilon}\left(\frac{1}{r_v}\right) dv \quad \text{eq (5)}$$

where $\varphi_s$ and $\varphi_v$ are the potential of the observation point; s is the area of the surface source; v is the volume of the volume source; $r_s$ and $r_v$ are the radial distance from the point of the source to the observation point; $\sigma_s$ and $\sigma_v$ are the impressed surface and volume charge density of the sources, respectively; $\sigma_{es}$ is the equivalent surface sources to be placed on the surface of boundaries and interfaces of different media.

Usually, $q_k$ , $\sigma_s$ and $\sigma_v$ in eq:3 to eq:5 are given and $\sigma_{es}$ is defined from the specified boundary conditions. The boundary conditions are discretized into individual elements referred to as boundary elements. The equivalent surface sources sustain these boundary conditions by a function which relates the location and magnitude of the sources to the boundary.

The equivalent surface source $\sigma_{es}$ is determined by eq:6,

$$\sigma_{es} = L^{-1} G \quad \text{eq (6)}$$

where $L^{-1}$ is the inverse of linear operator L which is determined by the geometry of the problem and G is a matrix determined by the boundary conditions. The method of weighted residuals is employed to solve eq:6.

The boundary conditions of potential (Dirichlet), nominal derivatives (Neumann), and the continuity of the flux density along the interface of different media are enforced. Once the sources are defined, the potential and electric field in the the problem domain can be determined by eq:2–eq:5 [9].

REFERENCES


[1] R. Hackam, "Outdoor HV composite polymeric insulators," IEEE Transactions on Dielectrics and Electrical Insulation, vol. 6, no. 5, pp. 557 – 585, 1999.

[2] R. Lings, EPRI AC Transmission Line Reference Book - 200 kV and Above, Third Edition, Third Edit. EPRI, 2005.

[3] C. Volat, M. Jabbari, M. Farzaneh, and L. Duvillaret, "New method for in live-line detection of small defects in composite insulator based on electro-optic E-field sensor," IEEE Transactions on Dielectrics and Electrical Insulation, vol. 20, no. 1, pp. 194–201, Feb. 2013.

[4] R. Zeng, Y. Zhang, W. Chen, and B. Zhang, "Measurement of electric field distribution along composite insulators by integrated optical electric field sensor," IEEE Transactions on Dielectrics and Electrical Insulation, vol. 15, no. 1, pp. 302–310, 2008.

[5] IEEE 644 , "IEEE Standard Procedures for Measurement of Power Frequency Electric and Magnetic Fields From AC Power Lines," 1994.

[6] M. S. Mirotznik and D. Prather, "How to choose EM Software," IEEE Spectrum, no. December, pp. 53–58, 1997.

[7] Y. Liao, S. Chyuan, and J. Chen, "FEM versus BEM," IEEE Circuits & Devices Magazine, no. October, pp. 25 – 34, 2004.

[8] Y. B. Yildir, "Three-Dimensional Electrostatic Field Analysis on the Microcomputer," ICWA Coil Winding Proceedings, 1989.

[9] T. Zhao and M. Comber, "Calculation of electric field and potential distribution along nonceramic insulators considering the effects of conductors and transmission towers," IEEE Transactions on Power Delivery, vol. 15, no. 1, pp. 313–318, 2000.

[10] B. Gunasekaran and P. Nirgude, "Optimization of grading rings for post insulators used in EHV/UHV transmission system," in IEEE 10th International Conference on the Properties and Applications of Dielectric Materials, 2012, pp. 0–3.